The Diffuse Interstellar Bands
Proceedings IAU Symposium No. 297, 2013
J. Cami & N. L. J. Cox, eds.

doi:10.1017/S1743921313015810

Blue Luminescence and Extended Red Emission: Possible Connections to the Diffuse Interstellar Bands

A. N. Witt

Ritter Astrophysical Research Center, University of Toledo, Toledo, OH 43606, USA

Abstract. Blue luminescence (BL) and extended red emission (ERE) are observed as diffuse, optical-wavelength emissions in interstellar space, resulting from photoluminescence by ultraviolet(UV)-illuminated interstellar grains. Faintness and the challenge of separating the BL and ERE from the frequently much brighter dust-scattered continuum present major observational hurdles, which have permitted only slow progress in testing the numerous models that have been advanced to explain these two phenomena. Both the ERE, peaking near 680 nm (FWHM $\sim 60-120$ nm) and the BL, asymmetrically peaking at ~ 378 nm (FWHM ~ 45 nm), were first discovered in the Red Rectangle nebula. Subsequently, ERE and BL have been observed in other reflection nebulae, and in the case of the ERE, in carbon-rich planetary nebulae, H II regions, high-latitude cirrus clouds, the galactic diffuse ISM, and in external galaxies. BL exhibits a close spatial and intensity correlation with emission in the aromatic emission feature at 3.3 micron, most likely arising from small, neutral polycyclic aromatic hydrocarbon (PAH) molecules. The spectral characteristics of the BL also agree with those of fluorescence by PAH molecules with 13 to 19 carbon atoms. The BL phenomenon is thus most readily understood as the optical fluorescence of small, UV-excited aromatic molecules. The ERE, by contrast, though co-existent with mid-IR PAH emissions, does not correlate with emissions from either neutral or ionized PAHs. Instead, the spatial ERE morphology appears to be strictly governed by the density of far-UV ($E \geqslant 10.5$ eV) photons, which are required for the ERE excitation. The most restrictive observational constraint for the ERE process is its exceptionally high quantum efficiency. If the ERE results from photo-excitation of a nano-particle carrier by photons with $E \geqslant 10.5$ eV in a single-step process, the quantum efficiency exceeds 100%. Such a process, in which one to three low-energy optical photons may be emitted following a single far-UV excitation, is possible in highly isolated small clusters, e.g. small, dehydrogenated carbon clusters with about 20 to 28 carbon atoms. A possible connection between the ERE carriers and the carriers of DIBs may exist in that both are ubiquitous throughout the diffuse interstellar medium and both have an abundance of low-lying electronic levels with $E \leqslant 2.3$ eV above the ground state.

Keywords. ISM: dust, ISM: lines and bands: ISM: individual: Red Rectangle

1. Introduction

Despite decades of observational, theoretical, and experimental research with focus on precise wavelengths, equivalent widths, polarization, and detailed profiles of diffuse interstellar bands (DIBs), a generally convincing identification of the carriers of this phenomenon has remained elusive. The search for further constraints on the nature of the DIB carriers has led over time to investigations of possible correlations with other poorly understood interstellar phenomena that are generally attributed to the smallest of interstellar grains, such as the far-ultraviolet extinction rise, the 2175 Å interstellar extinction bump (Witt *et al.* 1983; Seab & Snow 1984; Xiang *et al.* 2011), the mid-infrared aromatic emission bands (Salama & Allamandola 1994; Mulas *et al.* 2003), and the dust-related anomalous microwave emission (Iglesias-Groth 2008). Such studies were motivated by the

fact that the abundances of interstellar grains and molecules are tightly constrained by the cosmic abundances of the elements and the observed depletions from the gas phase (Snow & Witt 1995, 1996), especially for the crucial element carbon. It is, therefore, both likely and necessary that different interstellar phenomena are manifestations of the same carrier class. It is with this motivation that I want to examine whether the likely carriers of the optical dust luminescence phenomena Blue Luminescence (BL) and Extended Red Emission (ERE) could possibly be related to DIBs.

2. The Observation of ERE and BL

Despite the fact that both phenomena exhibit their spectral signatures in the optical wavelength range, ERE and BL were discovered comparatively late (Cohen *et al.* 1975; Schmidt *et al.* 1980; Vijh *et al.* 2004). Both forms of diffuse dust emission were discovered first in the proto-planetary Red Rectangle (RR) nebula, where ERE, peaking near 680 nm (FWHM $\sim 60-120$ nm), and BL, asymmetrically peaking at ~ 378 nm (FWHM ~ 45 nm), are exceptionally bright and the usually dominant scattered light continuum is exceptionally weak, thanks to an unfavorable scattering geometry.

The RR is powered by HD 44179, a binary consisting of a mass-losing post-AGB giant star and a mass-accreting solar-type main-sequence companion, hidden from direct observation by an optically thick, circum-binary dusty torus, which presents a nearly edge-on view to Earth-based observers. The dust in the RR is forming locally in the carbon-rich bi-conical outflow, driven by a jet arising from the accretion disk surrounding the secondary star (Witt *et al.* 2009; Thomas *et al.* 2013).

In the RR, the ERE is readily extracted by dividing the nebular spectrum by that of the illuminating star seen through scattering in the center of the nebula (Witt & Boroson 1990). The emission nature of the ERE is confirmed by a corresponding decrease in the linear polarization of the nebular light over the wavelength extent of the ERE band (Schmidt *et al.* 1980; Watkin *et al.* 1991) due to the dilution of the otherwise more strongly polarized scattered light. The BL was first detected by noting the partial filling-in of the hydrogen Balmer series absorption lines in the nebular spectrum when compared to the Balmer line profiles seen in the spectrum of HD 44179, the central star (Vijh *et al.* 2004). With observations of Balmer lines with upper states n = 4 to n = 13, a red-degraded profile with a peak at 378 nm emerges.

The spatial morphologies of the ERE and the BL in the RR are distinctly different (Vijh *et al.* 2005a, 2006). While the BL is brightest relative to the scattered light in the dark shadow regions cast outside the circum-binary torus in the RR, the ERE is predominantly confined to the narrow boundary region on the inner walls of the bi-cone of the outflow from the center. These are the regions that are most directly illuminated by the central source of the nebula (Schmidt & Witt 1991). The ERE is mainly responsible for the X-shape morphology of the RR, which is its identifying feature.

Subsequent to its discovery in the RR, ERE was observed extensively in reflection nebulae (Witt *et al.* 1984; Witt & Boroson 1990), planetary nebulae (Witt & Furton 1990, 1992), in H II regions (Perrin & Sivan 1992; Darbon *et al.* 1998, 2000), in the diffuse ISM at high galactic latitudes (Guhathakurta & Tyson 1989; Gordon *et al.* 1998; Szomoru & Guhathakurta 1998; Witt *et al.* 2008; Matsuoka *et al.* 2011), and in external galaxies (Perrin *et al.* 1995; Pierini *et al.* 2002).

Similarly, using the same technique that led to the detection of the BL in the RR, Vijh *et al.* (2005b) found BL in other reflection nebulae illuminated by early-type stars.

https://doi.org/10.1017/S1743921313015810 Published online by Cambridge University Press

3. Carriers of the BL

The BL is most likely the result of fluorescence by small, neutral PAH molecules with three to four aromatic rings, in particular the molecules anthracene, phenanthrene, and pyrene. This suggestion (Vijh *et al.* 2005a) is supported by several observed characteristics of the BL in the RR. These characteristics are:

(*a*) The BL spectrum closely matches the laboratory fluorescence spectra of these three molecules;

(*b*) the spatial morphology of the BL is very similar to that of the aromatic C-H stretch band at 3.3 micron (Kerr *et al.* 1999);

(*c*) the BL emitters distinctly prefer regions of the RR nebula that are shielded against direct illumination by the central source, and are missing where the UV field from the central source would lead to ionization of such molecules.

Theoretical models of the mid-infrared emission bands from neutral and ionized PAHs by Bakes *et al.* (2001) support this identification by showing that small neutral PAHs exhibit strong 3.3-micron bands, while these bands are not seen in the spectra of corresponding cations.

The identification of the BL spectrum with that of fluorescence by small, neutral PAHs does not, however, exclude the presence of larger PAHs and small, PAH-related molecules. Thomas & Witt (2006) showed that the gas-phase fluorescence spectrum of phenanthridine, a three-ringed PAH with a single nitrogen substitution, also provides an excellent fit to the BL spectrum. Furthermore, the gas-phase fluorescence spectrum of a mixture of similar quantities of both small and large PAHs is strongly dominated by the fluorescence by three- and four-ringed PAHs, which appear to have significantly higher fluorescence efficiencies than larger PAHs (Thomas & Witt 2006).

4. Constraints on the ERE Carrier

Most early attempts at identifying a likely carrier of the ERE have focused almost exclusively on matching the broad, featureless ERE spectrum. Among some of the rather diverse proposed candidates were hydrogenated amorphous carbon grains (HAC) (Witt & Schild 1988; Godard & Dartois 2010), quenched carbonaceous composites (QCC) (Sakata *et al.* 1992; Wada *et al.* 2009), the fullerene C_{60} (Webster 1993), silicon nanoparticles (Ledoux *et al.* 1998; Witt *et al.* 1998), PAH di-cations (Witt *et al.* 2006), and charged PAH clusters (Rhee *et al.* 2007). Obviously, many materials can produce photoluminescence in the red part of the spectrum, and additional, more discriminating constraints must be considered.

Fortunately, the observational record contains several such constraints.

(*a*) ERE is seen in many reflection nebulae, but it is absent in reflection nebulae with illuminating stars with $T_{\rm eff} < 10^4$ K (Darbon *et al.* 1999). This suggests that ERE is excited by far-UV photons and only far-UV photons, in contrast to ordinary photoluminescence, which is most readily excited by photons only slightly higher in energy than that of the emerging luminescence photons. This is confirmed by the ERE morphology in such objects as the RR (Vijh *et al.* 2006), the reflection nebulae NGC 2023 (Witt & Malin 1989), NGC 7023 (Witt *et al.* 2006), and the Pleiades (Kurth *et al.* 2013). In each instance, the ERE distribution is consistent with the radiative transfer of far-UV photons, originating in the illuminating sources and needed as the essential source of excitation.

(*b*) The wavelength of maximum ERE intensity shifts to longer wavelengths from near 600 nm to around 800 nm as the density of the exciting UV radiation field varies over

https://doi.org/10.1017/S1743921313015810 Published online by Cambridge University Press

nearly six orders of magnitude (Smith & Witt 2002). Simultaneously, the width of the ERE band doubles (Darbon *et al.* 1999). As the UV density of the illuminating radiation field increases by six orders of magnitude, the integrated ERE intensity increases by about four orders of magnitude (Smith & Witt 2002). These findings suggest that the ERE carrier is not a single molecule but rather consists of a family of marginally stable particles with a distribution of sizes. As the radiation density increases, the less stable, predominantly smaller carrier particles are destroyed, leading to a shift of the ERE maximum to longer wavelengths, accompanied by a lower overall conversion efficiency of far-UV photons into ERE photons.

(*c*) In a survey of 20 planetary nebulae, with equal numbers identified as either carbon-rich (C/O $>$ 1) or oxygen-rich (C/O $<$ 1), Furton & Witt (1992) detected ERE only in carbon-rich nebulae, none in oxygen-rich nebulae. Assuming that the dust seen in these objects is formed locally and reflects the chemical abundances seen in the nebular gas, this result suggests that the ERE carriers are carbonaceous in nature.

(*d*) The ERE is spatially not correlated with the emitters of the UIR emission bands, which are now widely attributed to a family of polycyclic aromatic hydrocarbon molecules, even though the two phenomena generally co-exist in the same sources. In particular, the ERE morphology in the Red Rectangle (Vijh *et al.* 2006) is distinctly different from that of of the 3.3-micron and 11.3-micron UIR band emission observed by Bregman *et al.* (1993). Similarly, the UIR emissions in the Spitzer/IRAC 8-micron band, the WISE 12-micron band, and the WISE 22-micron band in the Pleiades reflection nebulae have very different spatial distributions compared to that of the ERE, which reaches maximum intensity in the regions immediately surrounding the bright B stars in the Pleiades cluster, with highest ERE intensities near the most luminous Pleiades star, Alcyone (Kurth 2013). A similar lack of spatial correlation between ERE and UIR band emissions was noted by Perrin & Sivan (1992) in the Orion nebula, by Darbon *et al.* (2000) in the compact H II region Sh 152, and by Berné *et al.* (2008) in the NW PDR of the reflection nebula NGC 7023.

(*e*) The most severe constraint on the ERE process is imposed by the extremely high quantum efficiency inferred from the ERE intensity observed in the diffuse ISM at high galactic latitudes, where the intensity and spectrum of the illuminating radiation field are comparatively much better known than in nebulae illuminated by nearby stars with an uncertain geometric relationship. If claimed detections of ERE at high latitudes are accepted (Guhathakurta & Tyson 1989; Gordon *et al.* 1998; Szomoru & Guhathakurta 1998; Witt *et al.* 2008; Matsuoka *et al.* 2011; Ienaka *et al.* 2013), and if the standard interstellar Galactic radiation field in the solar vicinity (Mathis *et al.* 1983) is the source of its excitation, the photon conversion efficiency of the ERE process exceeds 100%, provided only photons with E $\geqslant$ 10.5 eV contribute to its excitation. This implies that typically one or two ERE photons would result from a single excitation by a far-UV photon. This would rule out any ordinary photoluminescence process with a theoretical maximum quantum efficiency of 100%.

5. Explanation of the ERE

Understanding the ERE has been challenging not so much in terms of finding plausible carriers that produce reasonable photoluminescence spectra resembling those seen in ERE sources, but rather in identifying a likely physical process that satisfies the exceptional constrains associated with the ERE phenomenon, summarized in the previous section. Interestingly, Léger *et al.* (1988) predicted such a fluorescence mechanism in highly isolated, large- or intermediate-size molecules, dubbed Poincaré fluorescence, well

https://doi.org/10.1017/S1743921313015810 Published online by Cambridge University Press

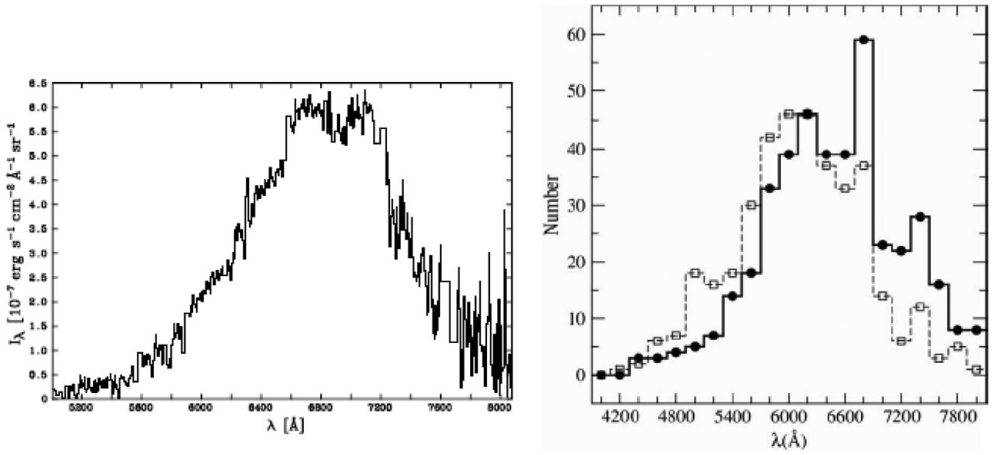

Figure 1. A comparison of a typical ERE spectrum observed in the NW PDR in the reflection nebula NGC 7023 (left image) with two histograms (right image) of the DIB density per unit wavelength, observed in the DIB surveys of Hobbs *et al.* (2008, 2009) toward HD 183143 (solid circles and solid line) and HD 204827 (open squares and dashed line).

before the most restrictive constraints for ERE were even known. This process is based on the concept of inverse electronic relaxation (Nitzan & Jortner 1979), which allows energy from highly excited vibrational levels of the electronic ground state to be transferred to energy levels of low-lying electronic excited states, as long as collisions with other particles do not occur before the fluorescence photons can be emitted. The process proceeds, because the transition probabilities for infrared stretching and bending modes are much lower than the transition probabilities for optical fluorescence transitions. The mechanism can produce more than a single fluorescence photon, provided the exciting photon is sufficiently energetic; thus, quantum efficiencies of 200% or even 300% are possible with ERE photon energies of $\sim$ 2 eV and exciting photons with E $\geqslant$ 10.5 eV, as indicated by the observational constraints. The required isolation conditions are easily met in interstellar space.

Duley (2009), starting from the concept of single-photon heating of small, isolated carbon clusters, arrives at a model for the ERE process that is identical to that proposed by Léger *et al.* (1988) in all essential details. Specifically, he proposes that ERE arises in dehydrogenated carbon clusters with between 20 and 28 carbon atoms, with quantum efficiencies between 200% and 300% for exciting photons in the range 10.5 eV $\leqslant$ E $\leqslant$ 13.6 eV, which are generally encountered in interstellar environments exposed to the interstellar radiation field. Carbon clusters with 20 to 28 atoms, including PAHs in this size range, are expected to be dehydrogenated (LePage *et al.* 2003; Montillaud *et al.* 2013) in environments where ERE is seen, thus providing a natural physical explanation for the lack of spatial correlations between ERE morphology and the distributions of UIR band emissions, generally attributed to PAHs.

Jones (1999) explored the relative stability of carbon clusters C_{2n} ($2 \leqslant n \leqslant 16$) and presented 60 stable isomers for the range ($10 \leqslant n \leqslant 14$) proposed by Duley (2009), including closed cages, monocyclic and bi-cyclic ring molecules, bowls, linear chains, and graphitic planar structures. Dehydrogenated PAHs appear to be less stable structures, while closed cages, including the smallest fullerene C_{20}, are among the most stable small carbon clusters, most likely to survive under interstellar conditions.

https://doi.org/10.1017/S1743921313015810 Published online by Cambridge University Press

6. Possible Connection of ERE to DIB Carriers

It is difficult to establish a direct correlation between the carriers of DIBs and the carriers responsible for the ERE, because DIBs are observed in absorption along the lines of sight toward distant stars, while ERE is seen as a diffuse emission phenomenon. A possible exception are the sharp emission bands seen in the spectrum of the Red Rectangle nebula, which may (Scarrott *et al.* 1999) or may not (Glinski & Anderson 2000) be the emission counterparts of DIBs occurring at nearly identical wavelengths (Van Winckel, these proceedings).

Despite these difficulties, it appears likely, however, that the carriers of DIBs and ERE are closely related families of particles with a substantial overlap. Both phenomena depend on particles that remain at least marginally stable in a wide variety of interstellar environments, in particular the diffuse interstellar medium. Both phenomena exhibit non-unique global spectra (Hobbs *et al.* 2008, 2009, Witt & Boroson 1990) indicative of families of numerous particles with a distribution that is sensitive to environmental factors such as the local radiation field. More specifically, both processes involve carriers with electronic states predominantly in the 1.4 eV to 2.2 eV range above the ground state. A histogram of the number of DIBs per unit wavelength interval (Hobbs *et al.* 2009) looks remarkably similar to a typical ERE spectrum, as illustrated in Figure 1, with a sharp rise longward of a wavelength of 540 nm and a broad peak in the 600 to 700 nm range. This indicates that the respective families of particles responsible for DIBs in absorption and for ERE in emission have essentially identical distributions of low-lying electronic states. It is possible that they are indeed truly identical.

Acknowledgements

I wish to thank the SOC for inviting me to speak at this very stimulating conference. Financial assistance in the form of a travel grant from the American Astronomical Society and a support grant from the International Astronomical Union are acknowledged with gratitude.

References

Cohen, M., *et al.* 1975, *ApJ*, 196, 179
Bakes, E. L. O., Tielens, A. G. G. M., & Bauschlicher, C. W. Jr. 2001, *ApJ*, 556, 501
Berné, O., Joblin, C., Rapacioli, M., Thomas, J, Cuillandre, J.-C., & Deville, Y. 2008, *A&A*, 479, L41
Bregman, J. D., Rank, D., Temi, P., Hudgins, D., & Kay, L. 1993, *ApJ*, 411, 794
Darbon, S., Perrin, J.-M., & Sivan, J.-P. 1998, *A&A*, 333, 264
Darbon, S., Perrin, J.-M., & Sivan, J.-P. 1999, *A&A*, 348, 990
Darbon, S., Zavagno, A., Perrin, J.-M., Savine, C., Ducci, V., & Sivan, J.-P. 2000, *A&A*, 364, 723
Duley, W. W. 2009, *ApJ*, 705, 446
Furton, D. G. & Witt, A. N. 1990, *ApJ*, 364, L45
Furton, D. G. & Witt, A. N. 1992, *ApJ*, 386, 587
Glinski, R. J. & Anderson, C. M. 2002,*MNRAS*, 332, L17
Godard, M. & Dartois, E. 2010, *A&A*, 519, A39
Gordon, K. D., Witt, A. N., & Friedmann, B. C. 1998, *ApJ*, 498, 522
Guhathakurta, P. & Tyson, J. A. 1989, *ApJ*, 346, 773
Hobbs, L. M., *et al.* 2008, *ApJ*, 680, 1256
Hobbs, L. M., *et al.* 2009, *ApJ*, 705, 32
Iglesias-Groth, S. 2008, *Organic Matter in Space, IAU Symp. 251*, 57
Ienaka, N., *et al.* 2013, *ApJ*, 767, 80

Jones, R. O. 1999, *J. Chem. Phys.*, 110, 5189
Kerr, T. H., Hurst, M. E., Miles, J. R., & Sarre, P. J. 1999, *MNRAS*, 303, 446
Kurth, M., Witt, A. N., Vijh, U. P., & Barnes, F. S. 2013, *AAS Mtg. #221*, #440.06
Ledoux, G., *et al.* 1998, *A&A*, 333, L39
Léger, A., Boissel, P., & d'Hendecourt, L. 1988, *PRL*, 60, 921
LePage, V., Snow, T. P., & Bierbaum, V. 2003, *ApJ*, 584, 316
Mathis, J. S., Mezger, P. G., & Panagia, N. 1983, *A&A*, 128, 212
Matsuoka, Y., Ienaka, N., Kawara, K., & Oyabu, S. 2011, *ApJ*, 736, 119
Montillaud, J., Joblin, C., & Toublanc, D. 2013, *A&A*, 552, A15
Mulas, G., Malloci, G., & Benvenuti, P. 2003, *A&A*, 410, 639
Nitzan, A. & Fortner, J. 1979, *J. Chem. Phys.*, 71, 3524
Perrin, J.-M. & Sivan, J.-P. 1992, *A&A*, 255, 271
Perrin, J.-M. & Sivan, J.-P. 1995, *A&A*, 304, L21
Pierini, D., Majeed, A., Boroson, T., & Witt, A. N. 2002, *ApJ*, 569, 184
Rhee, Y. M., Lee, T. J., Gudipati, M. S., Allamandola, L. J., & Head-Gordon, M. 2007, *PNAS*, 104, 5274
Sakata, A., *et al.* 1992, *ApJ*, 393, L83
Salama, F. & Allamandola, L. 1994, *The First Symposium on the Infrared Cirrus and Diffuse Interstellar Clouds*, ASP. Conf. Ser. 58, R. M. Cutri & W. B. Latter, Eds., 279
Scarrott, S. M., Watkin, S., Miles, J. R., & Sarre, P. J. 1992, *MNRAS*, 255, 11
Schmidt, G. D., Cohen, M., & Margon, B. 1980, *ApJ*, 239, L133
Schmidt, D. D. & Witt, A. N. 1991, *ApJ*, 383, 698
Seab, C. G. & Snow, T. P. 1984, *ApJ*, 277, 200
Smith, T. L. & Witt, A. N. 2002, *ApJ*, 565, 304
Snow, T. P. & Witt, A. N. 1995, *Science*, 270, 1455
Snow, T. P. & Witt, A. N. 1996, *ApJ*, 468, L65
Szomoru, A. & Guhathakurta, P. 1998, *ApJL*, 494, L93
Thomas, J. D., *et al.* 2013, *MNRAS*, 430, 1230
Thomas, J. D. & Witt, A. N. 2006, *Proc. of the NASA LAW 2006*, 264
Vijh, U. P., Witt, A. N., & Gordon, K. D. 2004, *ApJ*, 606, L65
Vijh, U. P., Witt, A. N., & Gordon, K. D. 2005a, *ApJ*, 619, 368
Vijh, U. P., Witt, A. N., & Gordon, K. D. 2005b, *ApJ*, 633, 262
Vijh, U. P., *et al.* 2006, *ApJ*, 653, 1336
Wada, S., Mizutani, Y., Narisawa, T., & Tokunaga, A. T. 2009, *ApJ*, 690, 111
Watkin, S., Gledhill, T. M., & Scarrott, S. M. 1991, *MNRAS*, 252, 229
Webster, A. 1993, *MNRAS*, 264, L1
Witt, A. N., Bohlin, R. C., & Stecher, T. P. 1983, *ApJ*, 267, L47
Witt, A. N. & Boroson, T. A. 1990, *ApJ*, 355, 182
Witt, A. N., Gordon, K. D., & Furton, D. G. 1998, *ApJ*, 501, L111
Witt, A. N., Gordon, K. D., Vijh, U. P., Sell, P. H., Smith, T. L., & Xie, R.-H. 2006, *ApJ*, 636, 303
Witt, A. N. & Malin, D. F. 1989, *ApJ*, 347, L25
Witt, A. N., Mandel, S., Sell, P. H., Dixon, T., & Vijh, U. P. 2008, *ApJ*, 679, 497
Witt, A. N. & Schild, R. E. 1988, *ApJ*, 325, 837
Witt, A. N., Schild, R. E., & Kraiman, J. B. 1984, *ApJ*, 281, 708
Witt, A. N., Vijh, U. P., Hobbs, L. M., Aufdenberg, J. P., Thorburn, J. A., & York, D. G. 2009, *ApJ*, 693, 1946
Xiang, F. Y., Li, A., & Zhong, J. X. 2011, *ApJ*, 733, 91